Suppressed formation of electron-hole droplets in diamond under a strain field

N. Naka, J. Omachi, and M. Kuwata-Gonokami
Department of Applied Physics, Graduate School of Engineering, The University of Tokyo, Tokyo 113-8656, Japan
(Received 29 September 2007; published 28 November 2007)

We present time-integrated and time-resolved photoluminescence spectra of excitons and electron-hole droplets in externally stressed diamond. A suppression of droplet luminescence and an enhancement of exciton luminescence are clearly observed due to the application of the strain field, reducing the degeneracy of the conduction bands. We observe that the application of a 1.1 GPa stress to the crystal results in a decrease of the critical temperature by approximately 10 K. Based on these results, we discuss the possibility to manipulate the quantum degenerate phases of an electron-hole ensemble at high density and low temperature.

DOI: 10.1103/PhysRevB.76.193202 PACS number(s): 78.47.+p, 71.30.+h, 71.35.Ee, 71.35.Lk

Many-body interactions play an essential role in determining the conditions for which an ensemble of carriers reaches a metallic or insulating state.[1] The study of metal insulator phase transitions (MITs) has been a central topic in solid state physics for the past few decades. An exotic material phase often appears near the MIT phase boundary in strongly correlated electron systems, such as a superconducting phase in transition metal oxides. Therefore, much work has been devoted to exploring the nature of MIT both theoretically and experimentally.[2] The appearance of novel critical phenomena near the MIT phase boundary provides some opportunities to realize highly sensitive functional materials. An electron-hole ensemble in optically pumped, indirect-gap semiconductors has been introduced as a suitable system to examine the MIT of quantum mechanical particles with a strong Coulombic interaction. Of particular interest has been the crossover between a Bose-Einstein condensate (BEC) of excitons and a metallic liquid state at low temperature and high density.[3] Systematic experiments so far on silicon and germanium, however, revealed a stabilized normal Fermi liquid state; neither BCS-type electron-hole condensate nor excitonic BEC phase appeared.[4] Recent attempts to realize an excitonic condensate by introducing repulsive exciton-exciton interaction in two-dimensional structures have brought renewed interest on this topic.[5–8]

Another route that may allow reaching a quantum degenerate state with ensemble of excitons is to destabilize the electron-hole liquid (EHL) phase by using an external field. Modification of the phase diagram in silicon and germanium by uniaxial stress application[9,10] and by nonuniform stress application[11,12] was reported in the 1970s to 1980s. One problem of the emission spectral analysis was the overlap of different recombination lines: EHL, plasma, free exciton, as well as biexciton lines within a narrow energy range of ~10 meV. Thus, there remained ambiguities on the phase diagram of stressed silicon analyzed from "poorly structured" spectra.[9] We revisit this problem to control the EHL phase by applying a strain field to diamond which is a wide indirect-gap semiconductor. Diamond has a much wider energy scale than silicon and germanium; therefore, spectral overlap is not problematic. In addition, following the recent development of ultrafast laser technology and advanced theoretical models[13] on nonequilibrium states of carriers, finding new hosts possessing material parameters that are completely different from silicon or germanium has become a pressing issue. In previous publications on diamond,[14,15] the appearance of a metallic phase as electron-hole droplets (EHDs) spatially separated from the excitonic gas was reported. Because diamond has high critical temperature and density and an extremely short electron-hole lifetime, it is well suited for the experimental investigation of dynamical many-body problems well below the critical temperature. As a next step to clarify similarities and differences with silicon and germanium, it is essential to demonstrate controllability of MIT (or an exciton Mott transition) or formation of liquid states. In this Brief Report, we demonstrate the control of the EHD phase in diamond by the application of a strain field. We succeeded in destabilizing the metallic phase and stabilizing a neutral excitonic phase. We have observed a drastic suppression of the EHD luminescence and an enhancement of the excitonic luminescence due to the applied strain field.

Figure 1(a) shows a schematic band diagram of diamond. The conduction band has sixfold minima along [100] axes.[16] In the figure, for illustrative purpose, we depict only three valleys, the [100] and $[\bar{1}00]$ ones in a superimposed way. The valence bands have a maximum at the Γ point. The spin-orbit splitting of the valence bands is negligibly small as compared to the Fermi energy E_{Fh} of holes, thereby making

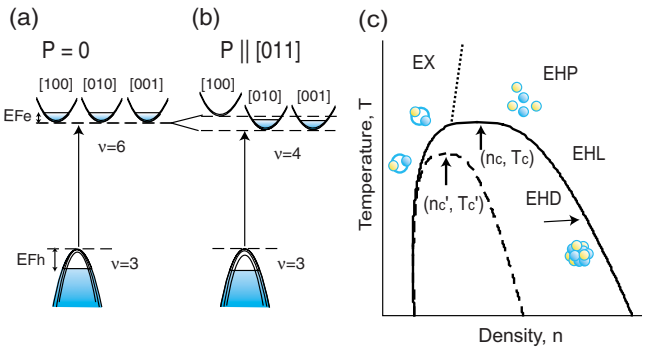

FIG. 1. (Color online) Schematic picture of the band structure of diamond (a) without and (b) with stress along a [011] axis. E_{Fe} and E_{Fh} denote Fermi energies of electrons and holes, respectively. (c) Phase diagram for unstressed (solid line) and stressed (dashed line) diamonds. EX, EHD, EHP, and EHL represent excitons, electron-hole droplets, electron-hole plasma, and electron-hole liquid, respectively. The upward arrows indicate the points for the critical condition for the formation of EHDs.

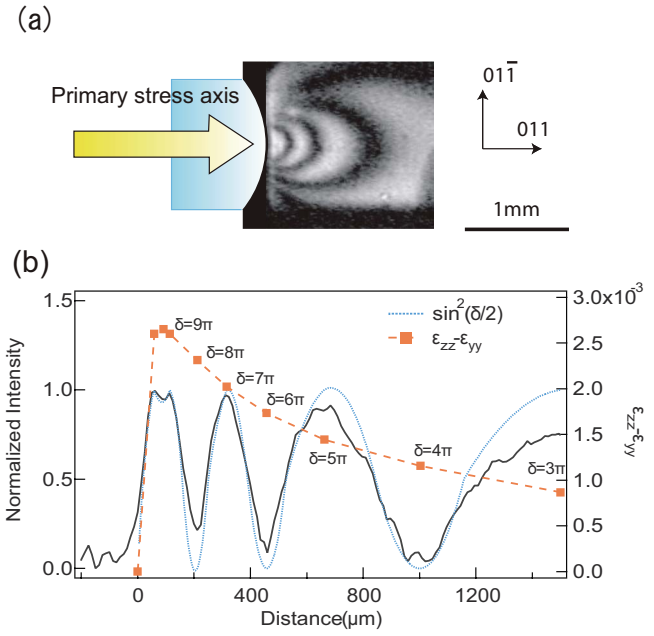

FIG. 2. (Color online) (a) Birefringence pattern taken under monochromatic light illumination. The fringes with orders of up to 4 are seen. The area of view is 1.7×1.8 mm^2. (b) Solid line, light intensity along the primary stress axis; solid squares, shear strain, $(\epsilon_{zz}-\epsilon_{yy})$, calculated by using Eq. (1). The maximum shear stress, $\tau=2.5$ GPa, occurs at 0.1 mm inside the sample surface. Dotted line: $\sin^2(\delta/2)$ calculated from δ's with interpolation.

the valence degeneracy to be virtually threefold. Under stress applied along the [011] axis, four valleys along the [010] and [001] axes lower the energy, as depicted in Fig. 1(b). This causes a lifting of the band degeneracy from sixfold to fourfold. The corresponding change in the phase diagram, as calculated from a microscopic theory presented in Ref. 9, is schematically shown in Fig. 1(c). The solid line represents the phase boundary of excitons (labeled EX) and EHL or electron-hole plasma (EHP) without stress. Inside the phase boundary, there is a coexisting region of EX and EHL, which we call EHD. The dashed line represents a case under finite stress. At the critical point (n_c, T_c), the lift of the band degeneracy may cause a drastic change of the properties of the electron-hole system. The EHD phase becomes more unstable, leading to the reduction of the critical density n_c and the critical temperature T_c.

We use colorless, type IIa single crystals of diamond synthesized by a high-temperature, high-pressure method. We apply a Hertzian stress with the primary stress axis along a [011] axis [see Fig. 2(a)]. The contact between the spherical plunger and the flat diamond surface leads to an inhomogeneous strain distribution.[17] We used an $R=1$ mm ball of tungsten carbide as the plunger. Figure 2(a) shows a birefringence pattern taken under monochromatic light illumination of a strained sample at 20 K between crossed polarizers. The polarizers are aligned so that the polarizations make an angle of ±45° to the primary stress axis. Diamond becomes biaxial under [011] compression.[18] The fringes are caused by the interference of ordinary and extraordinary waves.

According to the photoelastic theory,[19] the phase difference of the two waves passing through a diamond crystal deformed along a [001] axis is given by

$$\delta=\frac{\pi d}{\lambda}\kappa^{3/2}\sqrt{(p_{11}-p_{12})^2(\epsilon_{zz}-\epsilon_{yy})^2+4p_{44}^2\epsilon_{zy}^2}, \qquad (1)$$

where d and λ are the thickness of the crystal and the wavelength of the illumination light, respectively, and κ is the dielectric constant. Here, we assume that the strain tensor components ϵ_{ij} are homogeneous along the light path, because the curvature of the plunger and the extension of the strain distribution are much larger than d. In other words, we consider "effective" ϵ_{ij} averaged over the sample thickness. We neglect the strain component ϵ_{zy}, which is small along the primary stress axis, and take the values $d=0.5$ mm, $\lambda=610$ nm, $\kappa=5.7$,[20] and the piezo-optic constant $|p_{11}-p_{12}|=0.31$.[21] For the birefringence patterns, the intensity of the transmitted light is proportional to $\sin^2(\delta/2)$.

The solid line in Fig. 2(b) represents the measured light intensity along the primary stress axis. From the minima and maxima of this line, we quantify the phase δ as indicated in the figure. The solid squares are the shear strain, $(\epsilon_{zz}-\epsilon_{yy})$, calculated by solving Eq. (1) with these δ's. Since diamond is known to be very isotropic in terms of photoelasticity,[18] we use Eq. (1) for analysis of [011] compression. The dotted line indicates $\sin^2(\delta/2)$ calculated by interpolating points for δ's, which is comparable with the measured intensity (solid line). The slight deviation is due to the spatial inhomogeneity of the illuminated light intensity. We also estimate the magnitude of the shear stress, τ, by using an elastic relation $\tau=(\sigma_{zz}-\sigma_{yy})=(\epsilon_{zz}-\epsilon_{yy})/(s_{11}-s_{12})$ with compliance constants of $s_{11}=9.521\times10^{-4}$/GPa and $s_{12}=-9.920\times10^{-5}$/GPa.[22] The maximum shear stress is $\tau=2.5$ GPa at 0.1 mm inside the sample surface.

Figure 3(a) shows a typical photoluminescence spectrum of diamond at 124 K under zero stress. The light source is the fourth harmonics of Ti:sapphire laser light, at a wavelength of 202 nm. The pulse duration and the repetition rate are 200 fs and 1 kHz, respectively. The excitation light is focused on a spot of 40 μm diameter on the surface of the sample kept in a closed-cycle cryostat. The luminescence light is imaged onto the entrance slit of a monochromator (Acton, Spectra Pro 300i) by a pair of achromatic lenses. The detection was made by a liquid-nitrogen cooled charge coupled device camera (Princeton, LN/CCD-1100PB/UV).

The spectrum shows primary two components, the EHD (labeled EHD in the figure) and exciton (EX) components. The largest EHD line is due to TO-phonon assisted recombination. It takes on a broad bell-shaped line represented by an integral with Fermi distributions for electrons and holes. The red dashed line shows a simulated spectral shape assuming an EHD temperature of 133 K and a density of 8×10^{19} cm^{-3}. The maximum of the peak occurs at 5.18 eV. The line shapes of exciton components are represented by a Maxwell-Boltzmann distribution, $I_{ex}(E)=\sqrt{E}\exp(-E/k_BT_{ex})$, where E is the photon energy measured from the low-energy edges of the lines. To fit the measured spectra, we also include spectral broadening due to the resolution of the detection system by convoluting the Maxwell-Boltzmann distribu-

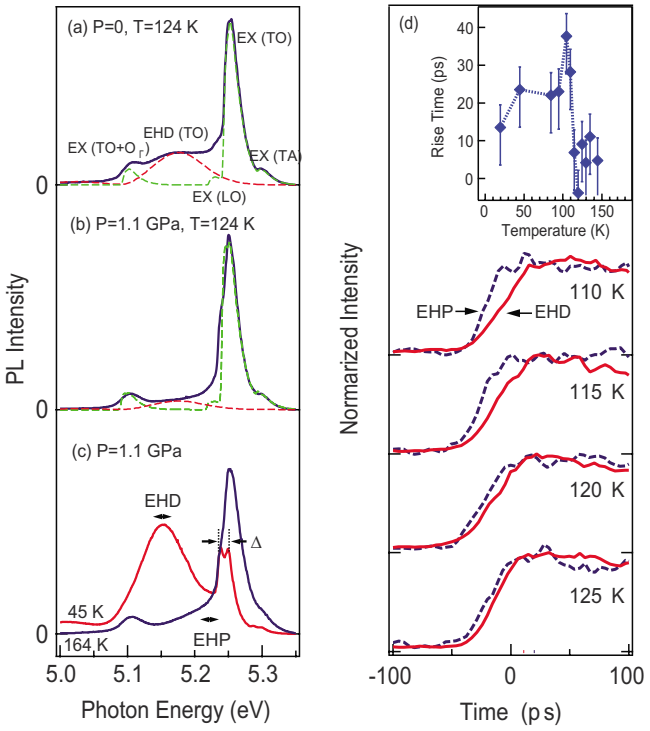

FIG. 3. (Color online) (a) TO-phonon assisted luminescence spectrum of excitons (EX) and EHD at 124 K without stress. Small peaks due to TA- and (TO+O_Γ)-phonon assisted recombination of excitons are also seen. The dashed lines are calculated spectra with parameters in text. (b) Spectrum with a 1.1 GPa stress. The shoulder below the TO-phonon assisted excitonic line is due to recombination of EHP. (c) Luminescence spectrum of stressed diamond at different temperatures. Δ indicates the separation of the split-off band under stress. Horizontal arrows indicate energy ranges for plotting EHD and EHP luminescence intensities in (d). (d) Temporal profiles of the EHD (solid line) and EHP (dashed line) components at different lattice temperatures, obtained by analyzing streak images. Inset: Temperature dependence of the rise time.

tion with a Gaussian function with a half-width of 3 meV. The green dashed line is the sum of contributions from TA-, TO-, LO-, and (TO+O_Γ)-phonon assisted recombination, with T_{ex}=133 K. The respective phonon energies are taken as 90, 141, 163, and 291 meV and intensity ratios 0.05:1:0.05:0.15.[15]

The solid curve in Fig. 3(b) is a spectrum taken at a position where a 1.1 GPa stress is applied. No distinct EHD line is seen because there is a broad luminescence ranging from 5.15 to 5.23 eV, which has been assigned as a recombination of the EHP.[15] Even though we exclude the existence of EHD based on the temporal analysis described below, for indicative purpose only, we show a maximum estimate of the EHD component with the red dashed line. As compared to the curve in Fig. 3(a), the ratio of EHD to exciton components is greatly suppressed, and the absolute intensity of the excitonic luminescence is increased. This is a clear indication that the EHD formation is suppressed and electron-hole pairs remain as excitons under a strain field.

The time-resolved measurements in Refs. 15 and 23 have demonstrated that the EHD luminescence appears several tens of picoseconds after the excitation laser pulse. This finite delay is a good method to distinguish EHD luminescence from EHP luminescence, which appears just after the laser pulse. Above the critical temperature, we expect no delay for luminescence at the photon energy for the EHD component. In order to know the critical temperature under stress, we carried out time-resolved measurements. The luminescence light was detected by a streak camera (Hamamatsu, M1955) mounted at the exit port of a 25 cm monochromator (Chromex, 250I). The temporal resolution was typically 40 ps.

For determining appropriate energy ranges for EHD and EHP luminescence, we show in Fig. 3(c) spectra in stressed diamond at lower and higher temperatures. At a lower temperature of 45 K, there is almost no EHP component. We find that the maximum of the EHD peak occurs at 5.15 eV, a slightly lower energy than in Fig. 3(a) due to a lowering of the split conduction bands by the strain, which can also be seen in the split Δ of the excitonic line. At a higher temperature of 164 K, the EHD component disappears and the EHP component shows up around 5.23 eV. Curves in Fig. 3(d) are temporal profiles of EHD and EHP components at different lattice temperatures. We plot luminescence intensities integrated over 5.14–5.16 eV for EHD and 5.21–5.23 eV for EHP as a function of time delay following the laser pulse. The inset shows the difference between rise times for the EHD and EHP components as a function of temperature. Up to 115 K, there is a clear delay for the EHD component. On the other hand, no delay is seen above 120 K. This indicates that the critical temperature is between 115 and 120 K. In the absence of a strain field, the critical point is at a lattice temperature of 132 K. Therefore, the change in the critical temperature by the stress application is (12±3) K.[24]

We now compare experimental values with theoretical expectations. Reductions of the critical temperature and density by a lift of the band degeneracy [Fig. 1(c)] can be understood in the following way. The critical density is proportional to the ground state density at which electron-hole pairs take the minimum energy E_0. This minimum energy, or so-called ground state energy, is linked to the critical temperature by the scaling law $E_0/(k_B T_c)$=const=9.3.[9,15] The lift of the degeneracy causes a decrease in the number of bands occupied by electrons at a given density, thereby making the kinetic energy larger, which has a positive contribution to the total energy. Thus, the total energy has a higher minimum point at a lower density. This implies reductions of the ground state energy, the ground state density, and the critical temperature.

In the Hertzian contact configuration, the stress is approximately uniaxial along the primary stress axis where we measure the change of the luminescence spectrum. Therefore, we expect that the conduction band degeneracy ν changes from 6 to 4 at high stresses. For simplicity, we assume a high-stress limit for the conduction bands and neglect the change or nonparabolicity of the valence band structure; for the mass parameters for diamond, we use an electron density-of-state mass of $\nu^{2/3} m_e = \nu^{2/3}(0.57 m_0)$ and a hole density-of-state mass of $0.91 m_0$,[25] where m_0 is the electron mass at rest. We estimate that the ground state density is reduced by 20% and that the corresponding change in the critical temperature is 8 K. The experimental values are in reasonable agreement.

To conclude, we have observed suppression of electron-hole droplet formation in stressed diamond. The Hertzian strain distribution was examined by observing birefringence patterns. The critical temperature was derived from the temperature dependence of rise times in the time-resolved spectral images. A decrease of the critical temperature by ~ 10 K was obtained with a 1.1 GPa applied stress, in reasonable agreement with a value estimated by a simple model assuming a high-stress limit in the [011] direction. The measurements we presented here were done at relatively high temperatures, where EHD lifetime is only in nanoseconds and the diffusion length is very small. Interesting future research directions may be to observe EHD condensation into a large droplet or to reveal ultrafast dynamics of nucleation. Stabilization of the excitonic phase, demonstrated in this study, is the first step toward excitonic Bose-Einstein condensation in indirect-gap semiconductors, which can be masked by an EHD phase in the absence of external fields. A complete lifting of the valence and conduction band degeneracies leads to a destabilization of the EHD phase (namely, EHD binding energy becoming smaller than the excitonic binding energy). This could be achieved by a combined application of strain and magnetic fields as was done in germanium.[26]

We thank K. Horiuchi (Tokyo Gas Co., Ltd.) for providing samples and M. Nagai for unpublished data and fruitful discussions. We also thank J. Benoit Heroux for critical reading of the Brief Report. This work was partially supported by CREST/JST and Special Coordination Funds for Promoting Science and Technology.

[1] N. F. Mott, Philos. Mag. **6**, 287 (1961).
[2] M. Imada, A. Fujimori, and Y. Tokura, Rev. Mod. Phys. **70**, 1039 (1998).
[3] P. Nozieres and S. Schmitt-Rink, J. Low Temp. Phys. **59**, 195 (1985).
[4] S. G. Tikhodeev, Sov. Phys. Usp. **28**, 1 (1985).
[5] T. Fukuzawa, E. E. Mendez, and J. M. Hong, Phys. Rev. Lett. **64**, 3066 (1990).
[6] L. V. Butov and A. I. Filin, Phys. Rev. B **58**, 1980 (1998); L. V. Butov, C. W. Lai, A. L. Ivanov, and D. S. Chemla, Nature (London) **417**, 47 (2002).
[7] V. Negoita, D. W. Snoke, and K. Eberl, Phys. Rev. B **60**, 2661 (1999).
[8] J. P. Eisenstein and A. H. MacDonald, Nature (London) **432**, 691 (2004).
[9] A. Forchel, B. Laurich, J. Wagner, W. Schmid, and T. L. Reinecke, Phys. Rev. B **25**, 2730 (1982).
[10] V. S. Bagaev, T. I. Galkina, O. V. Gogolin, and L. V. Keldysh, JETP Lett. **10**, 195 (1969).
[11] P. L. Gourley and J. P. Wolfe, Phys. Rev. B **24**, 5970 (1981).
[12] R. S. Markiewicz, J. P. Wolfe, and C. D. Jeffries, Phys. Rev. B **15**, 1988 (1976).
[13] J. H. Jiang, M. W. Wu, M. Nagai, and M. Kuwata-Gonokami, Phys. Rev. B **71**, 035215 (2005).
[14] K. Thonke, R. Schliesing, N. Teofilov, H. Zacharias, R. Sauer, A. M. Zaitsev, H. Kanda, and T. R. Anthony, Diamond Relat. Mater. **9**, 428 (2000).
[15] R. Shimano, M. Nagai, K. Horiuch, and M. Kuwata-Gonokami, Phys. Rev. Lett. **88**, 057404 (2002).
[16] M. Willatzen, M. Cardona, and N. E. Christensen, Phys. Rev. B **50**, 18054 (1994).
[17] S. P. Timoshenko and J. N. Goodier, *Theory of Elasticity* (McGraw-Hill, New York, 1970).
[18] C. B. Slawson and R. M. Denning, Am. Mineral. **40**, 1135 (1955); E. Poindexter, *ibid.* **40**, 1032 (1955); R. M. Denning, A. A. Giardini, E. Poindexter, and C. B. Slawson, *ibid.* **42**, 556 (1957).
[19] M. Yamada, Rev. Sci. Instrum. **64**, 1815 (1993).
[20] A. M. Zaitsev, *Optical Properties of Diamond* (Springer, Berlin, 2001).
[21] M. H. Grimsditch, E. Anastassakis, and M. Cardona, Phys. Rev. B **19**, 3240 (1979).
[22] M. H. Grimsditch and A. K. Ramdas, Phys. Rev. B **11**, 3139 (1975).
[23] M. Nagai, R. Shimano, K. Horiuchi, and M. Kuwata-Gonokami, Phys. Rev. B **68**, 081202(R) (2003).
[24] This value is slightly smaller than the difference of the lattice temperatures for the critical conditions with and without stress application because there is a tendency that an excitonic temperature is closer to the lattice temperature at higher temperature.
[25] R. Sauer, N. Teofilov, and K. Thonke, Diamond Relat. Mater. **13**, 691 (2004).
[26] V. D. Kulakovskii, I. V. Kukushkin, and V. B. Timofeev, Sov. Phys. JETP **54**, 366 (1981).